SUBMITTED TO THE ASTROPHYSICAL JOURNAL
Preprint typeset using LaTeX style emulateapj v. 10/09/06

MICROLENSING ZONE OF PLANETS DETECTABLE THROUGH THE CHANNEL OF HIGH-MAGNIFICATION EVENTS

CHEONGHO HAN
Program of Brain Korea 21, Department of Physics, Chungbuk National University, Chongju 361-763, Korea;
cheongho@astroph.chungbuk.ac.kr
Submitted to The Astrophysical Journal

ABSTRACT

A microlensing lensing zone refers to the range of planet-star separations where the probability of detecting a planetary signal is high. Its conventional definition as the range between ~ 0.6 and 1.6 Einstein radii of the primary lens is based on the criterion that a major caustic induced by a planet should be located within the Einstein ring of the primary. However, current planetary lensing searches focus on high-magnification events to detect perturbations induced by another caustic located always within the Einstein ring very close to the primary lens (stellar caustic) and thus a new definition of a lensing zone is needed. In this paper, we determine this lensing zone. By applying a criterion that detectable planets should produce signals $\geq 5\%$, we find that the new lensing zone varies depending on the planet/star mass ratio unlike the fixed range of the classical zone regardless of the mass ratio. The lensing zone is equivalent to the classical zone for a planet with a planet/star mass ratio $q \sim 3 \times 10^{-4}$ and it becomes wider for heavier planets. For a Jupiter-mass planet, the lensing zone ranges from 0.25 to 3.9 Einstein radii, corresponding to a physical range between ~ 0.5 AU and 7.4 AU for a typical Galactic event. The wider lensing zone of central perturbations for giant planets implies that the microlensing method provides an important tool to detect planetary systems composed of multiple ice-giant planets.

Subject headings: gravitational lensing

1. INTRODUCTION

The microlensing signal of a planet is a perturbation to the smooth standard light curve of the primary-induced lensing event occurring on a background source star. The planetary signal lasts for a short period of time: several days for a gas giant planet and several hours for an Earth-mass planet. Currently, the observational frequency of lensing surveys is ~ 1 per night and thus it is not enough to detect planetary signals. To achieve the observational frequency required to detect planetary signals, microlensing planet searches are using a combination of survey and follow-up observations. Survey observations (e.g., OGLE, http://www.astrouw.edu.pl/∼ogle, Udalski (2003); MOA, http://www.physics.canterbury.ac.nz/moa/, Bond et al. (2002a)) aim to maximize the event rate by monitoring a large area of the Galactic bulge field on a roughly nightly basis. They issue alerts of ongoing events in the early stage of lensing magnification by analyzing data in real time. Follow-up observations (e.g., PLANET, http://planet.iap.fr, Kubas et al. (2008); MicroFUN, http://www.astronomy.ohio-state.edu/%7Emicrofun/, Dong et al. (2006)) are focused on the alerted events in order to detect short-lived planetary signals.

In practice, however, the number of telescopes available for follow-up observations is far less for intensive followups of all alerted events and thus priority is given to those events which will maximize the planetary detection probability. Currently, the highest priority is given to high-magnification events (Bond et al. 2002b; Abe et al. 2004; Rattenbury et al. 2002). This is based on the fact that in addition to a major caustic located away from the primary lens (planetary caustic), a planet induces an additional tiny caustic in the region close to the primary lens (stellar or central caustic). Due to its location, the perturbations induced by the stellar caustic always occur near the peak of high-magnification events and this makes follow-up observations right on the period of greatest sensitivity possible. The strategy focusing on high-magnification events was proposed by Griest & Safizadeh (1998) and the adoption of the strategy has led to the discoveries of six planet candidates (OGLE-2005-BLG-071Lb, OGLE-2005-BLG-169Lb, OGLE-2006-BLG-109Lb,c, MOA-2007-BLG-400b, MOA-2007-BLG-192) among the total eight microlensing planet candidates discovered to date (Bond et al. 2004; Udalski et al. 2005; Beaulieu et al. 2006; Gould et al. 2006; Gaudi et al. 2008; Dong et al. 2008; Bennett et al. 2008).

In planetary microlensing, a 'lensing zone' refers to the range of planet-star separations where the probability of detecting a planetary signal is high. It was first discussed by Gould & Loeb (1992), who found that the planet detection probability is maximized when the planet is near the Einstein radius of the primary star. Later, the definition of the lensing zone is refined by Wambsganss (1997) and Griest & Safizadeh (1998) as the range between approximately 0.6 and 1.6 Einstein radii of the primary lens. In defining the lensing zone, the location of a caustic is important because perturbations can be covered by follow-up observations when they occur during the progress of the lensing magnification induced by the primary star.[1] When a planet is located within this range, not only the size of the planet-induced caustic is maximized but also the caustic is located inside the Einstein ring of the primary lens. However, this definition of the lensing zone is based only on the location of the planetary caustic. Considering that current lensing observations focus on perturbations induced by stellar caustics and these caustics are always located within the Einstein ring regardless of the

[1] We note that events are occasionally monitored in current follow-up observations even after the source has exited the Einstein ring. An example is the event OGLE-2005-BLG-390 (Beaulieu et al. 2006) for which the planet was detected at the moment when the source was about to exit the ring. For these events, the lensing zone is more extended and broader than the classical definition of the lensing zone.

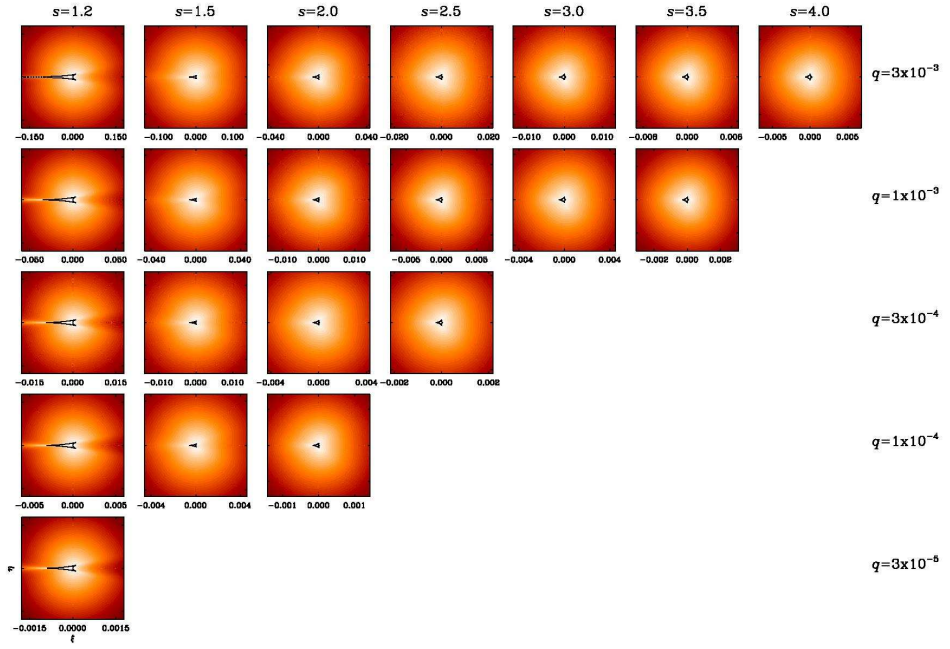

FIG. 1.— Maps of magnification pattern involved with a point source in the central region of planetary systems with various planet-star separations s and planet/star mass ratio q. The coordinates (ξ,η) represent the axes that are parallel with and normal to the planet-star axis, respectively. In each map, the star is at the center and the planet is on the left. The closed figures drawn in black curves represent the caustics. Greyscale is drawn such that brighter tone represents the region of a higher magnification.

planet-star separation, a new definition of the lensing zone is needed. In this paper, we determine the range of a lensing zone for microlensing planets detectable through the channel of high-magnification events.

The paper is organized as follows. In § 2, we briefly describe the properties of planet-induced caustics. In § 3, we investigate the patterns of lensing magnifications in the central region of planetary lens systems with various planet/star mass ratios and planet-star separations. From the investigation of the magnification pattern, we set the criterion for planet detections and determine the lensing zone based on this criterion. We discuss about the implication of the determined lensing zone. We summarize the result and conclude in § 4.

2. CAUSTICS OF PLANETARY LENSING

A planetary lensing corresponds to the case of binary lensing with a very low mass companion. One important characteristic of binary lensing is the formation of caustics. Caustics represent the set of source positions at which the magnification of a point source becomes infinite. For a planetary case, there exist two sets of disconnected caustics. One small stellar caustic is located near the primary star and the other planetary caustic is located away from the star.

The position vector to the center of the planetary caustic from the position of the primary lens is

$$\boldsymbol{\xi}_{pc} = \mathbf{s}\left(1-\frac{1}{s^2}\right), \tag{1}$$

where $\mathbf{s}$ is the position vector of the planet from the star normalized by the Einstein radius of the primary, $r_{\rm E}$. The Einstein radius is related to the physical parameters of the lens system by

$$r_{\rm E} \sim 3.8\ {\rm AU}\left(\frac{M}{0.3\,M_\odot}\right)^{1/2}\left(\frac{D_L}{6\ {\rm kpc}}\right)^{1/2}\left(1-\frac{D_L}{D_S}\right)^{1/2}, \tag{2}$$

where M is the mass of the primary lens and D_L and D_S are the distances to the lens and source star, respectively. Then, the planetary caustic is located within the Einstein ring for planets located in the range of

$$\frac{\sqrt{5}-1}{2} \le s \le \frac{\sqrt{5}+1}{2}. \tag{3}$$

This range corresponds to the lensing zone defined by Wambsganss (1997) and Griest & Safizadeh (1998). More details about the characteristics of planetary caustics are found in Han (2006).

The stellar caustic is smaller than the planetary caustic. Its size as measured by the width along the planet-star axis is related to the planet/star mass ratio q and planet-star separation s by

$$\Delta\xi_{cc} \sim \frac{4q}{(s-s^{-1})^2}. \tag{4}$$

The size of the stellar caustic decreases as $\propto q$, while the size of the planetary caustic decreases as $\propto q^{1/2}$. This implies that the stellar caustic shrinks more rapidly than the planetary caustic as the mass ratio decreases. In the limiting case of a very wide planet ($s \gg 1$) and a close-in planet ($s \ll 1$), the dependency of the size of the stellar caustic on the planet separation is

$$\Delta\xi_{cc} \propto \begin{cases} s^{-2} & \text{for } s \gg 1, \\ s^{2} & \text{for } s \ll 1. \end{cases} \tag{5}$$

For a given mass ratio, a pair of stellar caustics with separations s and s^{-1} are identical to the first order of perturbation approximation. Although the size depends both on q and s, the shape of the stellar caustic is solely dependent on the planet separation. For more detailed characteristics of stellar caustics, see Chung et al. (2005).

3. CENTRAL PERTURBATIONS

3.1. *Magnification Pattern*

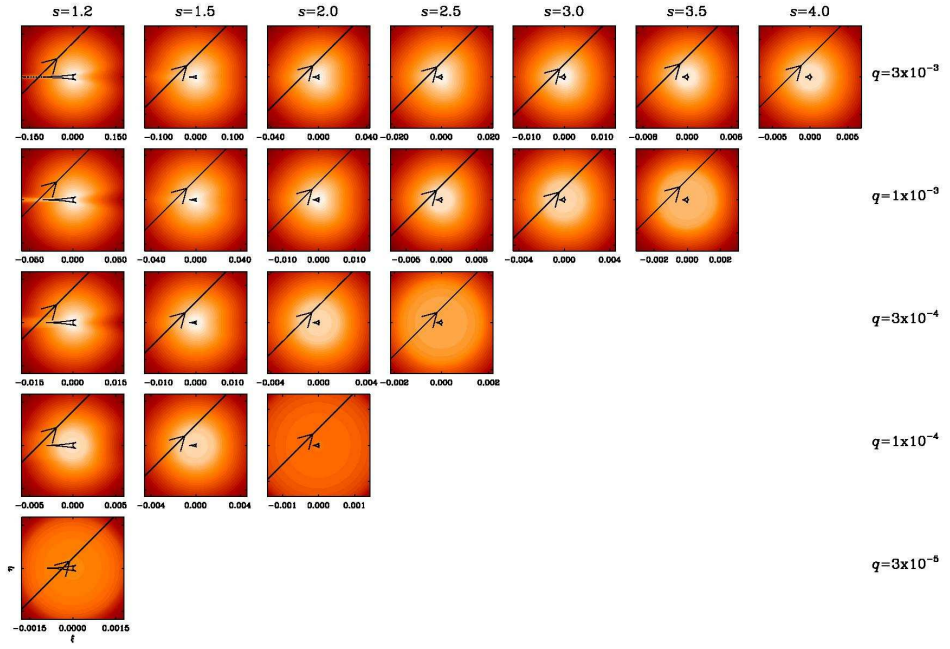

FIG. 2.— Magnification patterns with finite-source effect. Notations are same as in Fig. 1. The straight lines with arrows represent the source trajectories and the light curves of the resulting events are presented in the corresponding panels of Fig. 3.

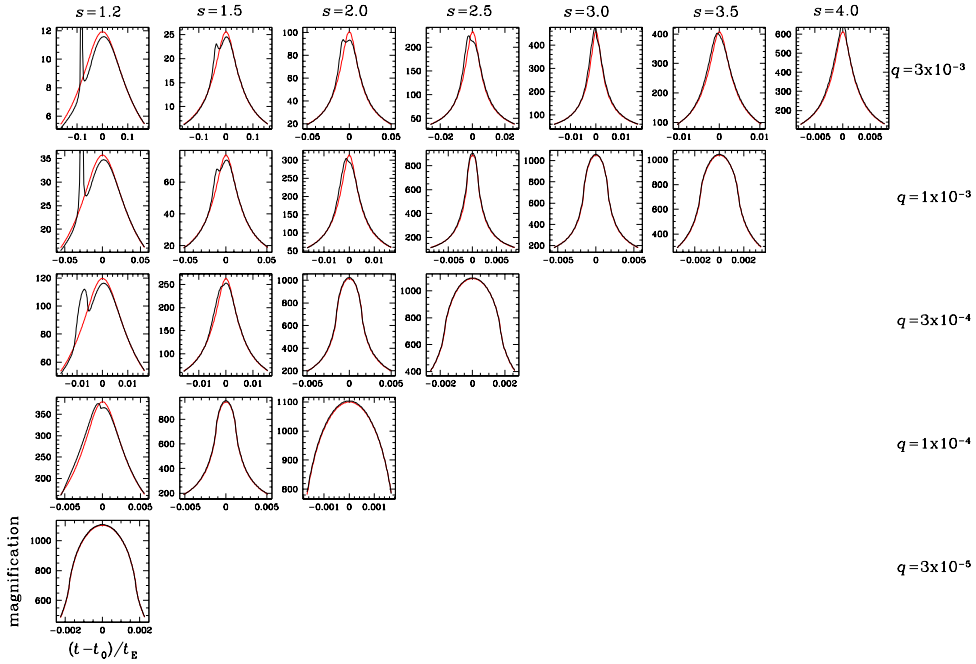

FIG. 3.— Example light curves of planetary lensing events with high magnifications. The lens systems and trajectories responsible for the individual light curves are presented in the corresponding panels in Fig. 2. Black and red curves are for events with and without the planet, respectively.

Since the stellar caustic is always close to the primary lens, its location can no longer be a criterion for the the determination of the lensing zone for planets detectable through the channel of high-magnification events. For these planets, the most important restriction on planet detection is the size of the caustic. If the caustic is too small, the perturbation produced by the caustic is severely washed out by the finite-source effect and thus cannot be detected (Bennett & Rhie 1996). Since the stellar caustic is small, perturbations induced by the stellar caustic are especially vulnerable to the finite-source effect.

To see how the finite-source effect affects planetary perturbations, we construct maps of magnification pattern in the central region of planetary systems with various mass ratios and separations. The constructed maps are presented in Figure 1 and Figure 2. For comparison, we present two sets of maps where the maps presented in Figure 1 are constructed not considering the finite-source effect, while those presented in Figure 2 are constructed by considering the effect. The finite-source effect is parameterized by the ratio of the source

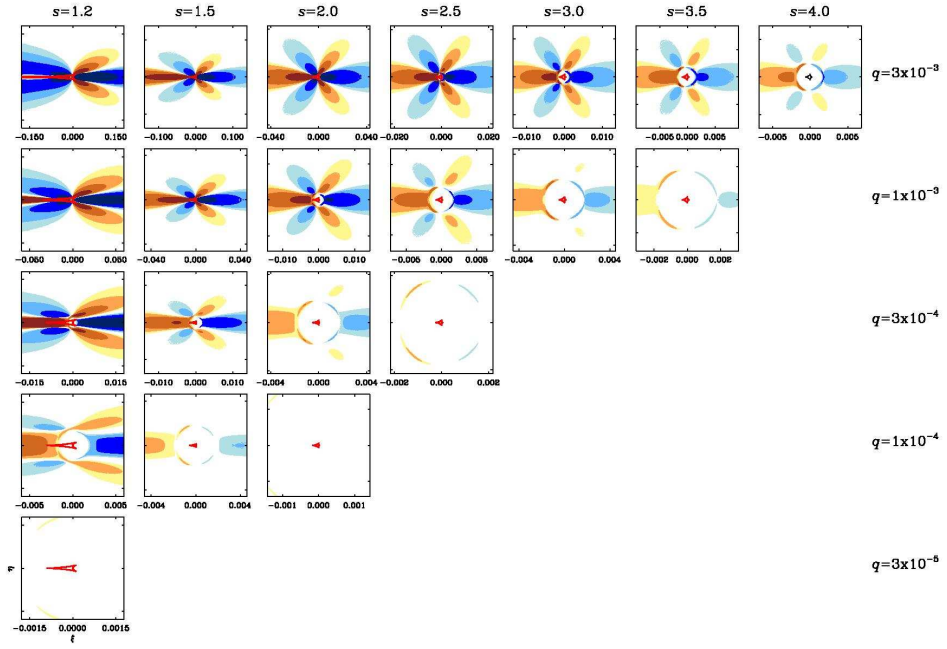

FIG. 4.— Maps of magnification excess ϵ. In each map, the regions with bluish and brownish colors represent the areas where the planetary lensing magnification is lower and higher than the single-lensing magnification, respectively. The individual colored areas represent the regions with $|\epsilon| \geq 2\%$, 3%, 5%, and 10%, respectively, with thickening tones of color.

radius, $r_\star$, to the Einstein radius of the primary lens. For Galactic bulge events, this ratio is scaled by the physical parameters of the lens system as

$$\rho_\star = 9\times10^{-4}\left(\frac{r_\star}{R_\odot}\right)\left[\left(\frac{M}{0.3\,M_\odot}\right)\left(\frac{D_L}{6\text{ kpc}}\right)\left(1-\frac{D_L}{D_S}\right)\right]^{-1/2}. \quad (6)$$

We consider the finite-source effect by assuming that the source star has a uniform disk with a radius equivalent to the sun and the physical parameters of the lens system are $M = 0.3\ M_\odot$, $D_L = 6$ kpc, and $D_S = 8$ kpc by adopting the values of a typical Galactic bulge event. This results in $\rho_\star = 1.8\times10^{-3}$. Then, the magnification affected by the finite-source effect becomes

$$A = \frac{\int_0^{\rho_\star} I(r)A_p(|\mathbf{r}-\mathbf{r}_L|)rdr}{\int_0^{\rho_\star} I(r)rdr}, \quad (7)$$

where $\mathbf{r}_L$ is the displacement vector of the source center with respect to the lens, $\mathbf{r}$ is the vector to a position on the source star surface with respect to the center of the source star, $I(r)$ represents the surface brightness profile of the source star, and A_p is the point-source magnification. We note that the blank space with missing panels in Figure 1 and Figure 2 implies that the magnification pattern is difficult to be distinguished from that of a single-lensing case. We also note that maps are presented only for the cases with $s > 1.0$ because the magnification patterns for a pair of planetary systems with s and s^{-1} are identical (Dominik 1999).

In Figure 3, we present example light curves of high-magnification events. The source trajectories responsible for the individual events are marked in the corresponding panels of Figure 2. In each panel, there are two light curves. One is for planetary lensing event (black curve) and the other is for a single-lensing event without the planet (red curve).

Also presented in Figure 4 are the maps of magnification excess, which represents the fractional deviation of the planetary lensing magnification A from the single-lensing magnification A_0, i.e.

$$\epsilon = \frac{A-A_0}{A_0}. \quad (8)$$

We note that the finite-source effect is taken into consideration for both A and A_0. In each excess map, the region with bluish colors represents the area where the planetary lensing magnification is lower than that of the single lensing, i.e. $\epsilon < 0$, while the region with brownish colors represents the area where the planetary lensing magnification is higher, i.e. $\epsilon > 0$. The individual colored areas represent the regions with $|\epsilon| \geq 2\%$, 3%, 5%, and 10%, respectively, with thickening tones of color.

3.2. *Lensing Zone*

The pattern of central perturbations depends both on the shape of the stellar caustic and its relative size to that of the source star. We conduct detailed investigation about the dependencies of perturbation pattern on the caustic shape and size. The results of this investigation are themselves very important for the understanding of central perturbations and thus we are preparing a separate paper for that. Although the detailed results of this work are not presented in this paper, several findings relevant to this work are (1) the dependency of the finite-source effect on the caustic shape is weak and (2) perturbations persist even when the caustic is substantially smaller than the source size. Specifically, we find that perturbations with $\epsilon \geq 5\%$ can be detected if the caustic is bigger than roughly one fourth of the source size (diameter), i.e., $\Delta\xi_{cc}/2\rho_\star \gtrsim 1/4$. This result is consistent with the case of a recently reported microlensing planet MOA-2007-BLG-400b that was discovered through the high-magnification channel (Dong et al. 2008). In this case, the caustic width is $\Delta\xi_{cc} = 0.0015$ and the source diameter is $2\rho_\star = 0.0064$ and thus the ratio of the caustic width to the source diameter is $\Delta\xi_{cc}/2\rho_\star \sim 0.23$. By adopting the criterion of planet detection as $\Delta\xi_{cc}/2\rho_\star \gtrsim 1/4$ and with the expression of the caustic

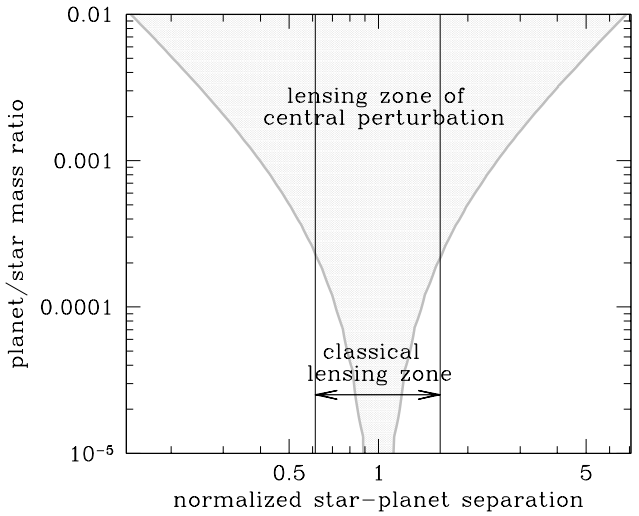

FIG. 5.— Lensing zone (shaded area) of planets detectable through the channel of high-magnification events in the parameter space of (s, q).

TABLE 1
LENSING ZONES

planet/primary mass ratio	lensing zone in normalized units	lensing zone in physical units
3×10^{-3}	$0.26 \lesssim s \lesssim 3.9$	0.5 AU $\lesssim d \lesssim$ 7.4 AU
1×10^{-3}	$0.40 \lesssim s \lesssim 2.5$	0.8 AU $\lesssim d \lesssim$ 4.8 AU
3×10^{-4}	$0.58 \lesssim s \lesssim 1.7$	1.1 AU $\lesssim d \lesssim$ 3.3 AU
1×10^{-4}	$0.72 \lesssim s \lesssim 1.4$	1.4 AU $\lesssim d \lesssim$ 2.6 AU
3×10^{-5}	$0.83 \lesssim s \lesssim 1.2$	1.6 AU $\lesssim d \lesssim$ 2.3 AU

NOTE. — Lensing zones of central perturbations for several example planets. The physical ranges are estimated by assuming a lens mass of $0.3\,M_\odot$.

size in equation (4), the condition for planet detection is

$$\frac{8q}{\rho_\star(s-s^{-1})^2} \gtrsim 1, \tag{9}$$

or equivalently,

$$s^2 - \sqrt{\frac{8q}{\rho_\star}}s - 1 \lesssim 0. \tag{10}$$

Solving this relation results in an analytic expression for the lensing zone of central perturbations of

$$\left|\sqrt{\frac{2q}{\rho_\star}} - \sqrt{\frac{2q}{\rho_\star}+1}\right| \lesssim s \lesssim \sqrt{\frac{2q}{\rho_\star}} + \sqrt{\frac{2q}{\rho_\star}+1}. \tag{11}$$

In Figure 5, we present the determined lensing zone (shaded area) in the parameter space of (s, q). From the comparison of the lensing zone of central perturbations with that of perturbations produced by planetary caustics, it is found that the lensing zone of central perturbations varies depending on the mass ratio unlike the fixed range of the classical lensing zone regardless of the mass ratio.[2] This is because while the position of the planetary caustic, which is the criterion for the classical lensing zone, does not depend on the mass ratio, the size of the stellar caustic, which is the criterion for the lensing zone of central perturbations, varies depending on the mass ratio. The dependency is such that a heavier planet has a wider lensing zone.

In Table 1, we list lensing zones for several cases of planets. We find that the lensing zone of central perturbations is equivalent to the classical lensing zone for a planet with a mass ratio $q \sim 3\times10^{-4}$. For planets with mass ratios greater than this, the lensing zone of central perturbations is wider than the classical lensing zone. For example, the lensing zone of a planet with $q = 3\times10^{-3}$, which corresponds to a Jupiter-mass planet around a low-mass star with $M \sim 0.3\,M_\odot$, ranges from $0.25 \lesssim s \lesssim 3.9$. In physical units, this range corresponds to 0.5 AU $\lesssim d \lesssim$ 7.4 AU for a typical Galactic bulge event. Considering the mass of the primary star, this lensing zone is equivalent to the range encompassing Mars to Uranus in our solar system when the dimension is scaled by the mass ratio of the lens to the sun.

The wider lensing zone of giant planets implies that microlensing method provides an important tool to detect planetary systems composed of multiple ice-giant planets. This is because all planets located within the lensing zone will produce their own signatures at a common area of the central perturbation (Gaudi, Naber, & Sackett 1998; Han 2005). In this sense, the recent discovery of a planetary system with a Jupiter/Saturn analog by the microlensing method (Gaudi et al. 2008) is not a fluke and we predict that microlensing will discover more of such multiple planetary systems in the future if they are common.

4. CONCLUSION

While the convention of defining the range of planet separation detectable by the microlensing method is based on the location of the planet-induced caustic, the range for planets detectable through the channel of high-magnification events cannot be defined by the conventional criterion because the caustic is always located close to the primary lens regardless of the planet separation. Instead, the most important restriction to the detection of central perturbation is given by the finite-source effect. We investigated the magnification pattern in the central region of various planetary systems and found that perturbations with $\geq 5\%$ can be detected if the caustic is bigger than roughly one fourth of the caustic size. Based on this finding, we derived an analytic expression for the range of planetary separations detectable through the central perturbations. From the comparison of classical lensing zone, we found that the new lensing zone is equivalent to the classical zone for a planet with a planet/star mass ratio $q \sim 3\times10^{-4}$ and it becomes wider for heavier planets. The wider lensing zone of the central perturbations for giant planets implies that the microlensing method provides an important tool to detect planetary systems composed of multiple ice-giant planets.

This work was supported by the Astrophysical Research Center for the Structure and Evolution of the Cosmos (ARCSEC) of Korea Science and Engineering Foundation (KOSEF) through Science Research Program (SRC) program.

[2] Strictly speaking, the lensing zone of perturbations induced by planetary caustics also depends on the mass ratio. This is because the planetary caustic has a finite size and thus part of the perturbation region induced by the caustic can be located within the Einstein ring even when the caustic center is outside the Einstein ring. The caustic size and the resulting perturbation region increase with the increase of the mass ratio and thus the lensing zone becomes broader as the mass ratio increases. However, we note that the caustic is small and thus this dependency is weak. For a planet with a mass ratio $q = 10^{-3}$, we find that this effect makes the lensing zone increase by $\sim 7\%$ assuming that the perturbation region extends 4 times of the caustic size.

REFERENCES

Abe, F., et al. 2004, Science, 305, 1264

Beaulieu, J. P., et al. 2006, Nature, 439, 437

Bennett, D. P., & Rhie, S. H. 1996, ApJ, 472, 660
Bennett, D. P., et al. 2008, ApJ, submitted
Bond, I. A., et al. 2002, MNRAS, 331, L19
Bond, I. A., et al. 2002, MNRAS, 333, 71
Bond, I. A., et al. 2004, ApJ, 606, L155
Chung, S.-J., et al. 2005, ApJ, 630, 535
Dominik, M. 1999, A&A, 349, 108
Dong, S., et al. 2006, ApJ, 642, 842
Dong, S., et al. 2008, in preparation
Gaudi, B. S., Naber, R. M., & Sackett, P. D. 1998, ApJ, 502, L33
Gaudi, B. S., et al. 2008, Science, 319, 927
Gould, A., & Loeb, A. 1992, ApJ, 396,
Gould, A., et al. 2006, ApJ, 644, L37
Griest, K., & Safizadeh, N. 1998, ApJ, 500, 37
Han, C. 2005, ApJ, 629, 1102
Han, C. 2006, ApJ, 638, 1080
Kubas, D., et al. 2008, A&A, 483, 317
Rattenbury, N. J., Bond, I. A., Skuljan, J., & Yock, P. C. M. 2002, MNRAS, 335, 159
Udalski, A. 2003, Acta Astron., 53, 291
Udalski, A., et al. 2005, ApJ, 628, L109
Wambsganss, J. 1997, MNRAS, 284, 172